European Journal of Pharmaceutics and Biopharmaceutics 136 (2019) 203–212

Contents lists available at ScienceDirect

European Journal of Pharmaceutics and Biopharmaceutics

journal homepage: www.elsevier.com/locate/ejpb

Research paper

Sortagged anti-EGFR immunoliposomes exhibit increased cytotoxicity on target cells

Steffen Wöll[a,c,*], Stephan Dickgiesser[b], Nicolas Rasche[b], Stefan Schiller[a], Regina Scherließ[c]

[a] Merck KGaA, Chemical and Pharmaceutical Development, Frankfurter Str. 250, 64293 Darmstadt, Germany
[b] Merck KGaA, ADCs & Targeted NBE Therapeutics, Frankfurter Str. 250, 64293 Darmstadt, Germany
[c] Department of Pharmaceutics and Biopharmaceutics, Kiel University, Grasweg 9a, 24118 Kiel, Germany

ARTICLE INFO

Keywords:
Sortase-A
Immunoliposomes
Bioconjugation
Targeted
Drug delivery
Epidermal growth factor receptor
Doxorubicin
Active targeting

ABSTRACT

Purpose: Conventional chemotherapy is associated with therapy-limiting side effects, which might be alleviated by targeted chemotherapeutics such as immunoliposomes. The targeting ligands of immunoliposomes are commonly attached by unspecific chemical conjugation, bearing risk of structural heterogeneity and therewith related biological consequences. Chemoenzymatic methods may mitigate such risks through site-specific conjugation.

Methods: The formulation parameters for pentaglycine–modified, doxorubicin–loaded liposomes and the reaction conditions for a site–specific, Sortase–A mediated conjugation with monoclonal antibodies were thoroughly evaluated. The cytotoxicity of such sortagged, epidermal growth factor receptor (EGFR)-specific immunoliposomes was tested on human breast cancer cells.

Results: Sortaggable liposomes with a defined size (140 nm, PDI < 0.25) and high encapsulation efficiency (> 90%) were obtained after manufacturing optimization. A ratio of 1.0–2.5 μM mAb/100 μM pentaglycine yielded stable dispersions and circumvented carrier precipitation during ligand grafting. The cytotoxicity on $EGFR^+$ MDA–MB–468 was up to threefold higher for EGFR–specific immunoliposomes than for the nontargeted controls.

Conclusions: Sortase–A is suitable to generate immunoliposomes with a site–specific ligand–carrier linkage and hence improves chemical homogeneity of targeted therapeutics. However, the sweet spot for manufacturability utilizing mAbs with two Sortase–A recognition sites is narrow, making mono-reactive binders such as scFvs or Fab's preferable for a further development. Despite this, the immunoliposomes demonstrated a targeted delivery of doxorubicin, indicating the potential to increase the therapeutic window during the treatment of $EGFR^+$ tumors.

1. Introduction

The major drawback of conventional anticancer drugs are dose-limiting adverse events that result in a narrowed therapeutic window. One strategy to overcome serious side effects is a targeted drug delivery, which leads to an accumulation of the drug in the tumor while omitting healthy tissues. Today, several concepts for targeted drug delivery have already successfully been applied, e.g. antibody-drug conjugates (ADCs) or drugs encapsulated in a targeted nanoparticulate carrier system such as immunoliposomes [1]. The latter requires the conjugation of a mostly proteinaceous ligand with an appropriate lipid anchor. For that, various chemistry-based coupling techniques, including maleimide–thiol conjugation with cysteines, amine condensation of lysines or N–hydroxysuccineimide-ester based coupling with carboxylic acid groups have been developed and have recently been extensively reviewed [2]. Although some immunoliposomal formulations have been clinically investigated [3–5], manufacturing hurdles and hence regulatory concerns remain high. Besides causing a tremendous effort in manufacturing a nano-sized drug carrier within the required specifications [6], chemistry-based conjugation methods additionally increase product heterogeneity [7]. Furthermore, stability of the linkers is a critical issue. Especially the widely used maleimide-linker can undergo a retro-Michael addition and exchange with albumin cysteine residues in vivo [8]. This includes cleavage between drug carrier and ligand, and thereby a loss of the targeting functionality. Site-specific, chemoenzymatic conjugation methods such as Sortase–A mediated transpeptidation have gained increasing interest for the synthesis of tailored antibody-drug conjugates (ADCs) [9]. The

* Corresponding author at: Merck KGaA, Chemical and Pharmaceutical Development, Frankfurter Str. 250, 64293 Darmstadt, Germany.
E-mail address: steffen.woell@merckgroup.com (S. Wöll).

https://doi.org/10.1016/j.ejpb.2019.01.020
Received 5 November 2018; Received in revised form 19 January 2019; Accepted 21 January 2019
Available online 21 January 2019
0939-6411/

enzyme–catalyzed modification of large protein structures at defined reaction sites leads to homogenous reaction products connected by a stable amide bond [10]. These reaction sites can be introduced by genetic engineering at uncritical parts of monoclonal antibodies such as the C–termini of the Fc part or constant domains of light chains [11]. This avoids the conjugation dependent decrease of antigen recognition in paratope regions observed after lysine-based conjugations [12], or a destabilization of antibodies during or after the reaction, as observed for cysteine conjugations [13,14]. Hence, deploying a chemoenzymatic method for the site-specific anchoring of targeting ligands would significantly improve the manufacturing process of immunoliposomes.

Doxorubicin (DXR) is a cytotoxic, DNA-intercalating anticancer agent with a broad applicability against many tumors, however also with a dose–limiting anthracycline induced cardiomyopathy as most severe adverse event [6,15]. The cardiotoxicity was alleviated by encapsulation of DXR into liposomal drug delivery systems [16]. This technology was commercialized as the "first nano-drug" Doxil®, developed by Barenholz and coworkers [6]. It is based on the efficient encapsulation of DXR by a remote loading technique [17], the use of high melting lipids together with cholesterol and finally a polyethylene glycol coating. Especially the latter leads to a prolonged circulation time and reduced uptake by the mononuclear phagocyte system (MPS) [6]. In addition to the reduced cardiotoxicity, compared to free DXR PEGylated liposomal DXR was found to accumulate to higher extents in human tumor effusions [18] or in human bone metastases of breast carcinoma than in adjacent muscle tissue [19]. This was interpreted as a passive drug targeting via the enhanced permeation and retention effect [6]. However, off-site effects such as mucositis or palmar-plantar erythrodysesthesia (skin toxicity) are still dose-limiting toxicities with PEGylated liposomal DXR [20]. This led to the approach of "active" targeting of liposomal DXR towards tumors by conjugation of tumor-specific ligands on the liposomal bilayer [1]. An established tumor target is the epidermal growth factor receptor (EGFR), whose overexpression is correlated with the pathogenesis of many tumors [21,22]. Treatments which utilize monoclonal antibodies (mAb) inhibiting the EGFR are efficacious and well-tolerated therapies [21,23]. One example is cetuximab (C225, Erbitux®), which is currently approved for the treatment of colorectal and head- and neck cancer. A sortaggable variant of cetuximab, on both heavy chains C–terminally conjugated via Sortase–A to the tubulin inhibitor monomethyl auristatin E (MMAE), was recently demonstrated to exhibit specific cytotoxicity on EGFR overexpressing cells [24]. This antibody was therefore regarded as suitable model binder to explore the site–specific Sortase–A conjugation technology on liposomes, with the aim to combine two established concepts – DXR loaded, PEGylated liposomes and the EGFR-specific mAb cetuximab. Therefore, we first thoroughly evaluated the manufacturing of pentaglycine modified, PEGylated liposomes by a continuous solvent injection process. We characterized the pentaglycine liposomes regarding liposome stability, doxorubicin loading and particle shape. Engineered monoclonal antibodies carrying a Sortase–A pentapeptide at their heavy chain C–termini specific for EGFR (C_H–LPETG–C225) or hen egg lysozyme (C_H–LPETG–aHEL) were conjugated to the pentaglycine liposomes. The chemoenzymatic transpeptidation was evaluated for reaction kinetics and physical stability of the reaction product. To investigate the in vitro targeting ability, the EGFR-specific immunoliposomes were tested for their toxicity on a human breast cancer cell line (MDA-MB-468).

2. Materials

Di-myristyl modified, PEGylated pentaglycine lipid DMA-PEG-G5 (structure shown in [25]) was obtained from Merck & Cie, Schaffhausen, Switzerland. 1,2-dipalmitoyl-sn-glycero-3-phosphocholine (DPPC), hydrogenated phosphatidylcholine from soybean (HSPC) and 1,2-distearoyl-sn-glycero-3-phosphoethanolamine-N-[methoxy(polyethylene glycol)-2000] (DSPE-mPEG) were acquired from Lipoid GmbH (Ludwigshafen, Germany). Dulbecco's phosphate buffered saline (DPBS, D1408), cholesterol, 4-(2-hydroxyethyl)piperazine-1-ethanesulfonic acid (HEPES) and Triton-X100 were obtained from Sigma-Aldrich (St. Louis, Missouri, USA). Ammonium sulfate and ethanol were obtained from Merck KGaA, Darmstadt, Germany. MilliQ water (Merck Millipore, Billerica, Massachusetts, USA) was used for preparation and analytical purposes. Doxorubicin was from Ark Pharma (Arlington Heights, Illinois, USA). Ca^{2+}–independent Sortase-A variant SortA7m and a single–domain antibody of camelid heavy chain only antibodies with one LPETG-motif (LPETG–VHH) were a kind gift of BioMed X GmbH, Heidelberg, Germany and prepared as described elsewhere [26].

3. Methods

3.1. Pentaglycine-liposome preparation

Liposomes were prepared by a continuous solvent injection process described in detail in [27]. In brief, DPPC, cholesterol, DSPE-mPEG and pentaglycine modified DMA-PEG-G5 (59.4:34.65:4.95:1, mol%) were dissolved to 90 mM in ethanol. The lipid solution was injected into 250 mM ammonium sulfate buffer pH 5.4 utilizing a binary pumping system combined with a custom–made T-piece at various flow rates. If DPPC was replaced by HSPC (as indicated in results), lipids were dissolved to 100 mM in ethanol and injected at 5 mL/min into 250 mM ammonium sulfate heated to 65 °C (40 mL/min). Buffer was exchanged to DPBS pH 7.4 or 10 mM HEPES pH 7.0 (as indicated in results) by tangential flow filtration (MicroKros® hollow fiber module, 500 kDa cut-off, 20 cm^2 filter area, Spectrum Labs, Los Angeles, CA, USA) to establish a pH and ammonium sulfate gradient over the liposomal membrane [28].

3.2. Liposome characterization

The hydrodynamic diameter and polydispersity index (PDI) were measured by dynamic light scattering (DLS) using a DynaPro Plate Reader II (Wyatt, Santa Barbara, California, USA). The liposome dispersion was diluted to 3% (v/v) with surrounding buffer to achieve measurable count rates. The zeta potential (zp) was assessed using a Zetasizer Nano ZS (Malvern Instruments, Worcestershire, UK) after a dilution in 10 mM NaCl to 3% (v/v). Content of each lipid component was determined by a rp–HPLC method with an evaporative light scattering detector as described earlier [25]. The lipid stability of pentaglycine-modified liposomes was evaluated over an eight weeks storage at 2–8 °C.

Differential scanning calorimetry (DSC1, Mettler Toledo, Columbus, Ohio, USA) was used to determine the transition temperature of the liposomal bilayer. Aqueous lipid slurries (100–200 mg/mL) were prepared by 30 min hydration of preformed lipid films in an ultrasound bath. 100 µL of slurry was transferred to 160 µL aluminum pans. Pans were covered with a pierced lid. DSC measurement was performed with a temperature profile of 5 min equilibration at 5.0 °C; followed by a heating step (5 K/min) to 75 °C, a plateau phase at 75 °C for 3 min and return to 5 °C (-20 K/min). Two cycles were applied per sample, second cycle was used to calculate the melting temperature.

3.3. Doxorubicin loading and quantification

To screen DXR loading into the liposomes, DXR (10 mg/mL in water) and liposomes were mixed to a lipid-to-DXR ratio of 5:1 (m/m). In some cases, 10 × DPBS stock was added to adjust salt concentration to 1 × DPBS as indicated in the results. The liposomes were incubated for 30 min – 24 h in 1.5 mL tubes in an Eppendorf Thermomixer Comfort heating block (1000 rpm, 49 °C). Afterwards, the dispersion was immediately transferred into dialysis bags (Slide-A-Lyzer, MWCO 10 kDa, Thermo Fisher, Waltham, Massachusetts, USA) and dialyzed for at least 24 h with five buffer changes against DPBS pH 7.4 until the

concentration of DXR in the dialysis buffer was < 0.2 μg/mL. DXR content was determined as follows: liposomal samples were diluted in 5% Triton X–100 (v/v) and incubated for 30 min at 50 °C to ensure a complete vesicle lysis with subsequent dequenching of the encapsulated DXR. Fluorescence intensity (excitation: 485 nm, emission 595 nm) was measured in a 96-well plate reader (M200, Tecan Group, Männedorf, Switzerland) and DXR was quantified using a calibration row in lysis medium (0.06–2 μg/mL). The method typically showed good linearity ($r^2 > 0.999$), accuracy (95–105% of individually prepared 1 μg/mL samples) and specificity as lipid matrix had negligible influence on DXR quantification.

Lipid and DXR content was used to calculate the encapsulation efficiency (EE) according to Eq. (1).

$$EE\ [\%] = 100 * \frac{\frac{c(DXR)}{c(Lipid)}(after\ \ dialysis)}{\frac{c(DXR)}{c(Lipid)}(during\ \ loading)} \quad (1)$$

3.4. Recombinant expression and purification of monoclonal antibodies

Antibodies for Sortase–A mediated conjugation (C_H–LPETG–mAb) were manufactured using established recombinant expression and purification procedures. Briefly, mammalian expression vectors encoding for EGFR-specific C225 (cetuximab) and a hen egg lysozyme (aHEL)-specific IgG1 fused to a Sortase–A recognition motif (LPETGS) at their heavy chain C-termini were synthesized by GeneArt (Thermo Fisher Scientific, Waltham, MA, USA). Antibodies were recombinantly expressed in transiently transfected mammalian cells for five days using Expi293 expression system (Thermo Fisher Scientific, Waltham, MA, USA) and afterwards purified from the supernatant by protein A affinity chromatography.

3.5. Ligand conjugation: Reaction conditions and kinetic monitoring

Chemoenzymatic Sortase-A transpeptidation was used to conjugate C_H–LPETG–mAbs to pentaglycine modified liposomes. The reaction behavior was investigated by spiking different concentrations of C_H–LPETG–C225 to the DXR-LS (100 μM pentaglycine, from which roughly 50 μM were expected to be accessible at the outer leaflet of the bilayer). The mixture was equilibrated at 4 °C, and hydrodynamic diameter, PDI and attenuation-corrected light scattering count rate were determined using a Zetasizer Nano ZS. Detection angle was set to 173° (back scatter), data was analyzed via cumulants fit. After addition of 25 μM Sortase-A, the colloidal stability was tracked during the transpeptidation reaction over 4 h to determine feasible reaction conditions. To further evaluate reaction kinetics and endpoint, 1 μM C_H–LPETG–aHEL, DXR free liposomes (100 μM pentaglycine) and 25 μM Sortase–A were incubated at 4 °C. 5 μL of the mixture were sampled in 30 min intervals and analyzed by an rp-HPLC-DAD method published earlier for the analysis of single-domain antibody conjugation to pentaglycine-lipids [27]. The chromatographic conditions, namely the column temperature (60 °C) and the flow rate (1 mL/min) were modified to achieve sharp protein elution. This led to separation of Sortase-A, unmodified C_H–LPETG–aHEL and with one ((DMA–-PEG)–C_H–LPETG–aHEL) or two ((DMA–PEG)$_2$–C_H–LPETG–aHEL) lipid anchors modified mAb variants. The reaction progress was calculated as the relative area of each species from the area of 1 μM unmodified C_H–LPETG–aHEL at 280 nm (Eq. (2), s_n – species of interest; t_i – actual time point; A – peak area; A_0 – area of 1 μM C_H–LPETG–aHEL). At this wavelength, the influence of amide bonds being introduced by the pentaglycine-modified lipid was negligible. The total sum of the areas of the different mAb species during the reaction did never deviate to more than 6% from the mean area of a 1 μM C_H–LPETG–aHEL standard (n = 3, each injected in triplicate). The double-banded peak of mono-modified mAb was treated as single species.

$$reaction\ \ progress\ \ [\%]\ \ of\ \ s_n = \frac{A_{s_n}(t_i)}{A_0} \quad (2)$$

Liposome batches for in vitro cytotoxicity experiments were conjugated with 1 or 2.5 μM of C_H–LPETG–aHEL or C_H–LPETG–C225 for 4 h at 4 °C to DXR-loaded liposomes (DXR loading: 4 h at 49 °C, incubation in DPBS buffer), followed by dialysis in Float-A-Lyzer devices (MWCO 1000 kDa, G235037, Spectrum Labs, Los Angeles, California, USA). In case of HSPC-based liposomes, DXR had been loaded for 1 h at 65 °C from 10 mM HEPES buffer pH 7.0. Liposome-bound mAb concentration was calculated from the peak area of both (DMA–PEG)–C_H–LPETG–mAb and (DMA–PEG)$_2$–C_H–LPETG–mAb after analysis with above described rp-HPLC method using a 2.5 μM sample of non-lipidated C_H–LPETG–mAb as reference.

3.6. Cryo transmission electron microscopy

Cryo transmission electron microscopy (cryo–TEM) studies were done according to a method described by Klaiber and colleagues [29]. In brief, a thin sample film stretched over the lace holes of a hydrophilized carbon grid was shock frozen by rapid immersion in liquid ethane (97 K). Microscopic examinations utilized a Zeiss/LEO EM922 Omega EFTEM (Zeiss Microscopy GmbH, Jena, Germany) operated at an acceleration voltage of 200 kV and a temperature of 95 K. Images were taken and processed by a digital camera and software system (Gatan, München, Germany).

3.7. In vitro cytotoxicity

Cytotoxicity of EGFR- and HEL-targeted liposomes (the latter used as an isotype control) was tested on EGFR-positive cells (MDA-MB-468). 10,000 cells were seeded in 80 μL growth medium (RPMI supplemented with 10% fetal calf serum, 2 mM L-glutamine and 1 mM Na–pyruvate) in 96–well plates and incubated overnight at 5% CO_2 and 37 °C in a humidified atmosphere. Dilution series of antibody-modified formulations or control groups were prepared in medium and added to the cells, spanning a final DXR concentration from 100 μg/mL to 1.2×10^{-4} μg/mL (5.5fold dilution series, 9 concentrations tested). Wells with cells but without test compound as well as without cells were included as controls. Wells were incubated for 4 h at 37 °C, carefully washed three times with 125 μL fresh medium each and incubated for another 3 days in 100 μL fresh medium. Finally, cell viability was assessed by using CellTiterGlo® luminescent cell viability assay (Promega, Madison, WI, USA) according to the manufacturer's instructions. Data was normalized using wells with cells but without test compound as 100% and those without cells as 0%. IC_{50} values and statistics were determined by fitting to a 4-parameter regression model with GraphPad Prism software (GraphPad Software, La Jolla, CA, USA).

4. Results and discussion

4.1. Liposomal formulation development

Sortaggable, pentaglycine modified liposomes were prepared by a continuous and scalable solvent injection process utilizing a binary pumping system and a T–shaped mixing element as described earlier [27]. Buffer flow rate was screened for influence on hydrodynamic diameter (d_h) and PDI (Fig. 1). Mean size was reduced with increased buffer flow due to increased shear forces at the injection site [30].

Compared to previously reported manufacturing processes, slightly larger (20 nm) d_h were obtained in ammonium sulfate buffer compared to DPBS [27], although other manufacturing parameters (lipid composition and molarity; organic solvent, flow rates) were equal. This indicates the influence of buffer type on the liposome formation mechanism or on the bilayer appearance. Here, lipid headgroups may interact with salts or change their protonation status due to different pH,

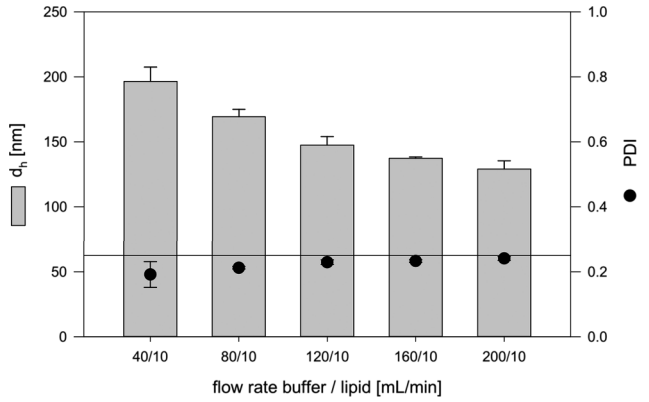

Fig. 1. Liposomal size adjustment. The total flow rate was varied to optimize the hydrodynamic diameter (d_h) and polydispersity index (PDI) of the liposomal dispersion obtained from lipid injection into 250 mM ammonium sulfate buffer. Mean size was adjustable between 200 and 130 nm, PDI was < 0.25 (reference line) for all settings.

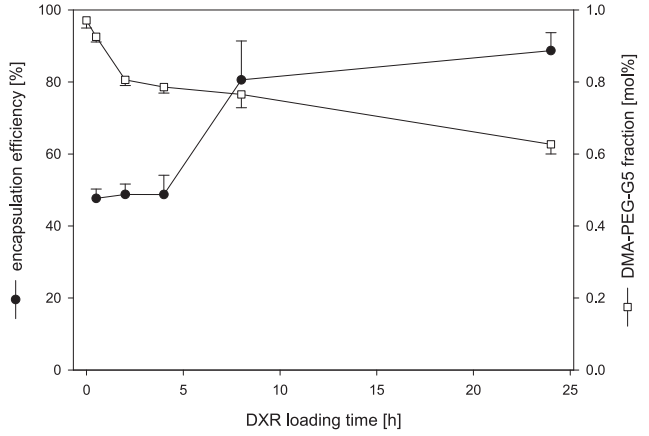

Fig. 2. Doxorubicin loading to pentaglycine modified, PEGylated liposomes. Encapsulation efficiency was low for short incubation times ≤ 4 h and increased up to 89% after a 24 h loading. The amount of DMA-PEG-G5 in the bilayer concomitantly decreased with prolonged loading at elevated temperature (49 °C), indicating a thermodynamic lability of this amino acid lipid. Data is shown as mean ± standard deviation of loading experiments with three liposome batches.

leading to a change of their headgroup volume. PDI was < 0.25 for all settings, what indicates an acceptable polydispersity of the dispersion. A buffer flow rate of 120 mL/min was chosen for further experiments to prepare liposomes with a mean size of ≈150 nm. This size was previously shown as suitable for effective targeting of myeloid immune cells in vitro [27] and in vivo [31] with equally composed pentaglycine liposomes. Tangential flow filtration was used to exchange the surrounding buffer to DPBS and to concentrate the liposomal dispersion. These pH and ammonium sulfate gradient pentaglycine liposomes were stable at 2–8 °C for eight weeks regarding physical parameters (size, PDI, zeta potential; Supplementary Fig. 1). Furthermore, the liposomes were found to be chemically stable as the bilayer composition was maintained during storage (Supplementary Fig. 2). Active loading of drugs to liposomes via a pH and salt gradient typically requires heating to the transition temperature (t_m) of the bilayer [28]. t_m of the lipid blend including the pentaglycine lipids was therefore determined by DSC (Supplementary Fig. 3). The measured t_m of 43.7 ± 1.8 °C was comparable to the t_m of the major component DPPC (t_m = 41 °C [32]). As expected, the t_m was not altered by the integrated DMA–PEG–G5 in a relevant manner compared to previous studies. Therefore loading experiments were conducted at 49 °C [28]. DXR loading duration was evaluated by dialyzing aliquots drawn from the loading bulk after different time points (Fig. 2) in a dialysis bag (10 kDa membrane cut–off). This molecular weight cut–off was suitable to ensure sufficient permeability for the small molecule DXR (543.5 Da). Surprisingly, after lipid and DXR content determination, low encapsulation efficiencies (< 50%) were obtained for short loading times up to 4 h (Fig. 2).

This was an unexpected result, as typical encapsulation efficiencies for doxorubicin via ammonium sulfate remote loading procedure are > 90% [6]. We therefore further increased the loading time, achieving encapsulation efficiencies of 89 ± 5% after 24 h, however with significant impact on chemical and physical stability of the liposomes. DMA-PEG-G5 bilayer fraction decreased upon long lasting incubation at 49 °C, indicating a temperature sensitivity of this lipid (Fig. 2). Furthermore, liposome size and PDI increased with continuing incubation (Supplementary Fig. 4).

We hypothesized, that the loading buffer was the reason for initially low encapsulation efficiencies. A phosphate buffer was used to obtain a liposomal dispersion ready for Sortase–A conjugation, similar to a previously described protocol for liposome modification [27]. Phosphate salts are known to form a gel-like, viscous dispersion with DXR [33,34]. This may hinder an efficient and fast DXR diffusion through the liposome membrane, thereby increasing the required time for an exhaustive loading. This was supported by an inverse correlation of loading efficiency and absolute phosphate concentration in the loading mix (Supplementary Fig. 5), resulting from different mixing ratios of the DPBS-surrounded liposome dispersion and the aqueous DXR stock solution. Further increases of loading efficiency were observed when an additional dialysis step was added after TFF, most likely by an enhancement of the salt and pH–gradient by a reduction of ammonium sulfate residuals. These small solutes may underlie a quick reverse diffusion over the TFF–membrane (molecular weight cut–off: 500 kDa) [35], hampering an efficient ammonium sulfate gradient generation. The additional dialysis step prior to DXR loading increased the encapsulation efficiency to 93% at a phosphate concentration of 0.58 mM (4 h incubation).

Cryo–TEM was used to image the liposomes individually after solvent injection, tangential flow filtration and doxorubicin loading (Fig. 3). Mostly spherical, uni- to bilamellar vesicles were observed after injection and tangential flow filtration. DXR loading had dramatic effects on the liposome appearance: different from frequently reported “coffee-bean” or “rugby” structures [17], many liposomes had a rod–-like appearance, probably due to a subsequent growing doxorubicin precipitate in the liposome interior. These rod-like, drug-loaded liposomes had lengths of several hundred nanometers. Furthermore, “donut”-like structures were observed. The precipitate inside the vesicles had a fibrous appearance with a periodicity of about 3 nm, comparable to previous descriptions of such liposomes being loaded via the ammonium sulfate method [36]. Though partly present already after solvent injection and TFF, plenty of disk-like micelle structures were observed especially after doxorubicin-loading. Lasic et al. suggested that the presence of DSPE–mPEG stabilized these flat structures [36,37]. Subsequent processing such as tangential flow filtration and DXR loading may enhance their formation by increased stress factors like shearing during pumping and elevated temperature during loading. Thus, we investigated whether loading time or loading medium may influence the liposome appearance. While reduction of the incubation to 1 h did not lead to a homogenous dispersion (Fig. 3E), exchanging the loading medium from DPBS to HEPES buffer (as frequently described by various groups [33,38–41]) had considerable influence on the liposome appearance (Fig. 3F). Typical coffee-bean structures were obtained by this method and less rod-like structures were observed. Interestingly, though liposomes appeared quite different in cryo–TEM, dynamic light scattering measurements did not indicate such distinct differences (Supplementary Table 1). It remains unclear why the loading medium has such a high impact on the precipitate dimension inside the vesicles. There might be a co-diffusion of a doxorubicin-

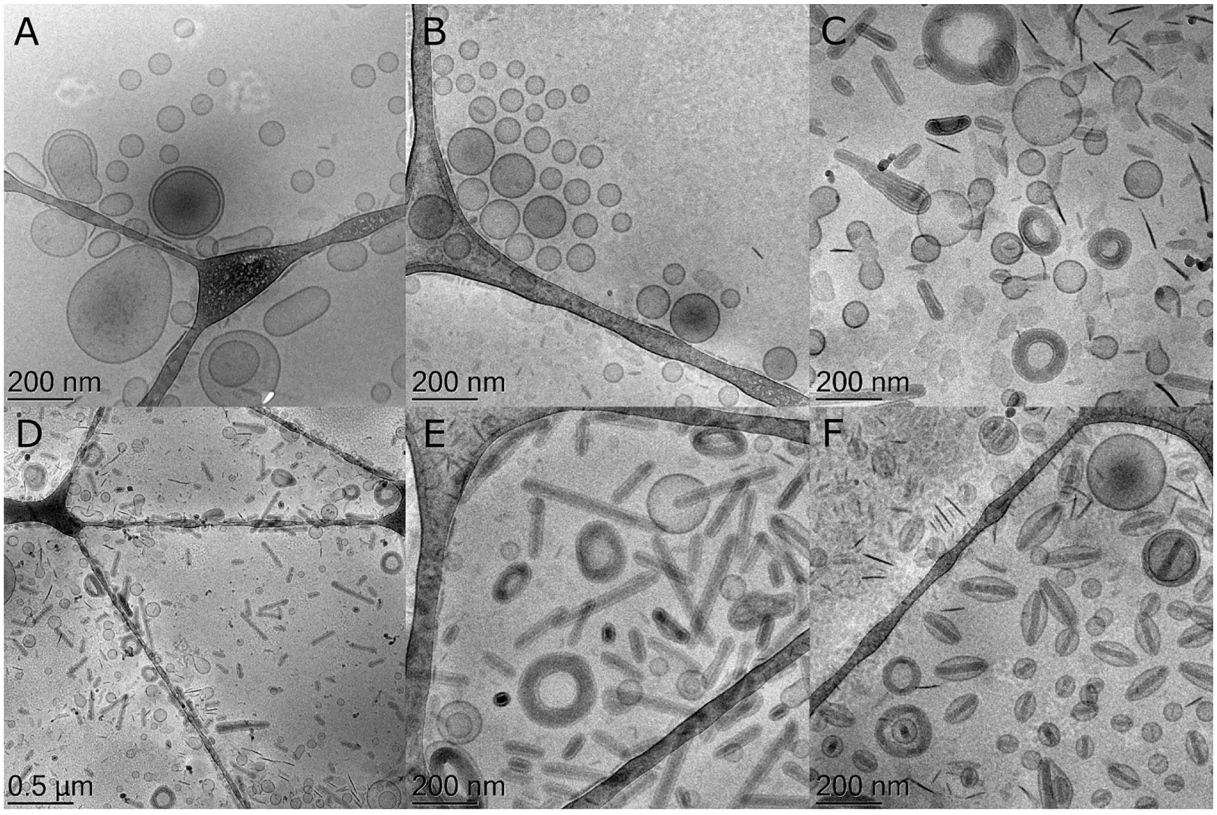

Fig. 3. Representative cryo–TEM pictures of pentaglycine liposomes prepared by solvent injection. A: after solvent injection in ammonium sulfate buffer; B: after rebuffering to DPBS; C and D: after DXR loading (4 h incubation, from DPBS); E: after DXR loading (1 h incubation, from DPBS); F: after DXR loading (1 h incubation, from HEPES buffer).

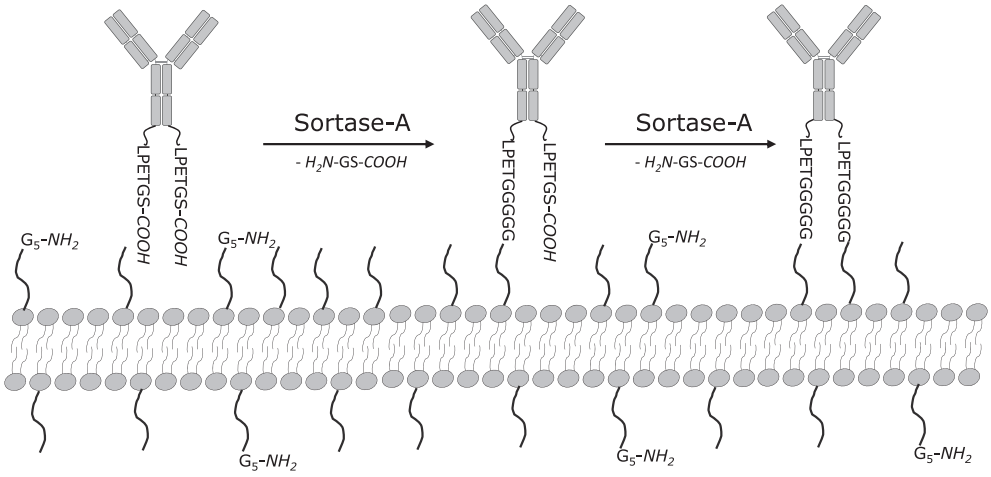

Scheme 1. Schematic conjugation of C_H–LPETG–mAb onto a PEGylated, pentaglycine modified bilayer.

phosphate salt inside the liposome interior during the loading at elevated temperature, or slight phosphate "loading" during the shearing caused by the peristaltic pump during TFF. Presence of different anions in the liposome interior are known to have significant impact on the appearance of the precipitate [42]. Low concentrations of phosphate anions inside the liposomes may therefore influence DXR precipitate morphology, thereby leading to the observed rod-like structures.

4.2. Ligand conjugation

Sortase-A was used to graft C_H–LPETG–mAbs on the pentaglycine modified liposomal surface (Scheme 1). This enzyme promotes a transpeptidation between the threonine of the LPETG stretch and the N-terminal amino group of the pentaglycine lipid anchor. Since the LPETG-motif was C-terminally attached to both heavy chain C-termini of the homodimeric antibody, two modifications per C_H–LPETG–mAb were distinguishable (mono–modification, termed as (DMA–-PEG)–C_H–LPETG–mAb, and a di–modification, termed as (DMA-PEG)$_2$-C_H–LPETG–mAb).

Both expected conjugate species were observed as separate peaks in a rp–HPLC analysis (Fig. 4). Liposomes equivalent to 100 µM pentaglycine, from which roughly 50 µM were estimated to be accessible for the reaction due to their presence on the outer leaflet of the bilayer (assuming an even distribution in the layers), were incubated with

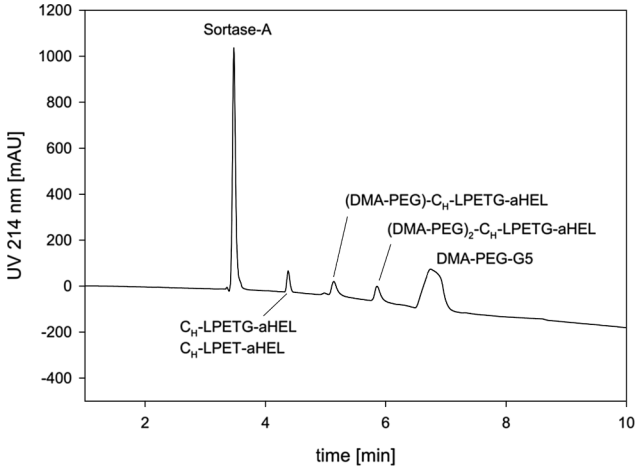

Fig. 4. rp–HPLC analysis of Sortase-A mediated C_H–LPETG–aHEL conjugation to pentaglycine-modified liposomes. Reaction conditions: Sortase-A (25 μM), C_H–LPETG–aHEL (1 μM) and liposomes (100 μM based on pentaglycine content); incubated for 2 h at 4 °C.

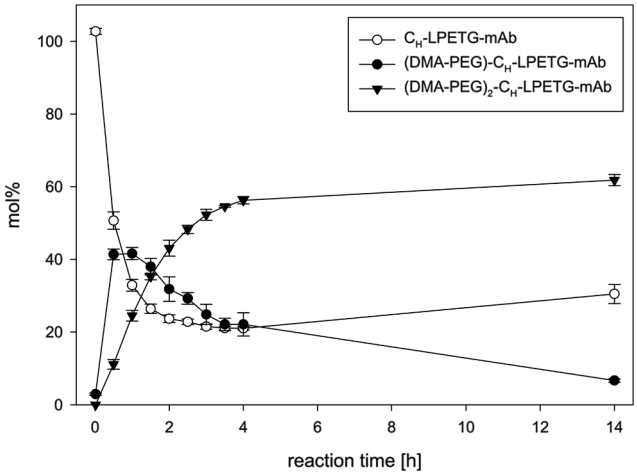

Fig. 6. Kinetics of Sortase–A (25 μM) mediated conjugation of C_H–LPETG–aHEL (1 μM) to pentaglycine-modified, PEGylated liposomes. The mono-modified (DMA-PEG)–C_H–LPETG–aHEL is the major product for up to 1.5 h incubation, after which the di-modified (DMA-PEG)$_2$-C_H–LPETG–aHEL is the dominant fraction. A significant reverse reaction can be observed between 4 h and 14 h, indicated by an increase of the non-lipidated C_H–LPETG–aHEL fraction in the terminal reaction phase. The maximum amount of aHEL conjugated to the liposomes (sum of mono- and di-modified mAb) was observed after 4 h (78.4 mol %).

various concentrations of C_H–LPETG–C225. Since macroscopically visible precipitation occurred with initially used high ratios of C_H–LPETG–C225 towards the liposomes (50 μM C_H–LPETG–C225 to 100 μM total pentaglycine), we systematically screened reaction conditions for a stable conjugation protocol (Fig. 5).

For that purpose, a cuvette-based dynamic light scattering measurement was deployed and the laser light attenuation corrected ("derived") count rate was used as a parameter for colloidal stability. Here, sedimentation of insoluble aggregates decreases the optical density of the sample in the measurement zone of the cuvette. Monitoring of the derived count rate clearly showed a correlation between the initial C_H–LPETG–C225 concentration and the colloidal stability. The count rate decreased drastically for 25 and 5 μM initial C_H–LPETG–C225 concentration. Only in case of very low C_H–LPETG–mAb concentrations (1 μM), a completely stable reaction was observed, indicated by an unchanged count rate, d_h and PDI. The d_h increased especially for the higher concentrations of 5 and 25 μM, followed by a decrease down to ≈100 nm due to aggregation and sedimentation. The PDI followed a similar behavior for those two concentrations applied. Liposomes modified with 2.5 μM C_H–LPETG–C225 showed an intermediate behavior. Although the derived count rate decreased significantly for this group, no changes in mean size or PDI were observed. This indicates the formation of a fraction of insoluble and sedimenting aggregates, which are not suitable to be detected by DLS, since they are typically considered as dust by DLS algorithms. Hence, they do not contribute to calculation of the d_h or PDI. Control groups including pure liposomes, a sample of liposomes and 25 μM C_H–LPETG–C225 without Sortase–A as well as a mixture of liposomes, 50 μM LPETG–VHH and Sortase–A did not show aggregation (Supplementary Fig. 6). The mass ratio of protein to lipid was similar for the reaction conditions of 50 μM VHH and 5 μM C_H–LPETG–C225. Potentially, the dual mAb modification results in a cross linking of liposomes via Sortase–A and is thereby responsible for the high aggregation propensity at increased antibody concentrations.

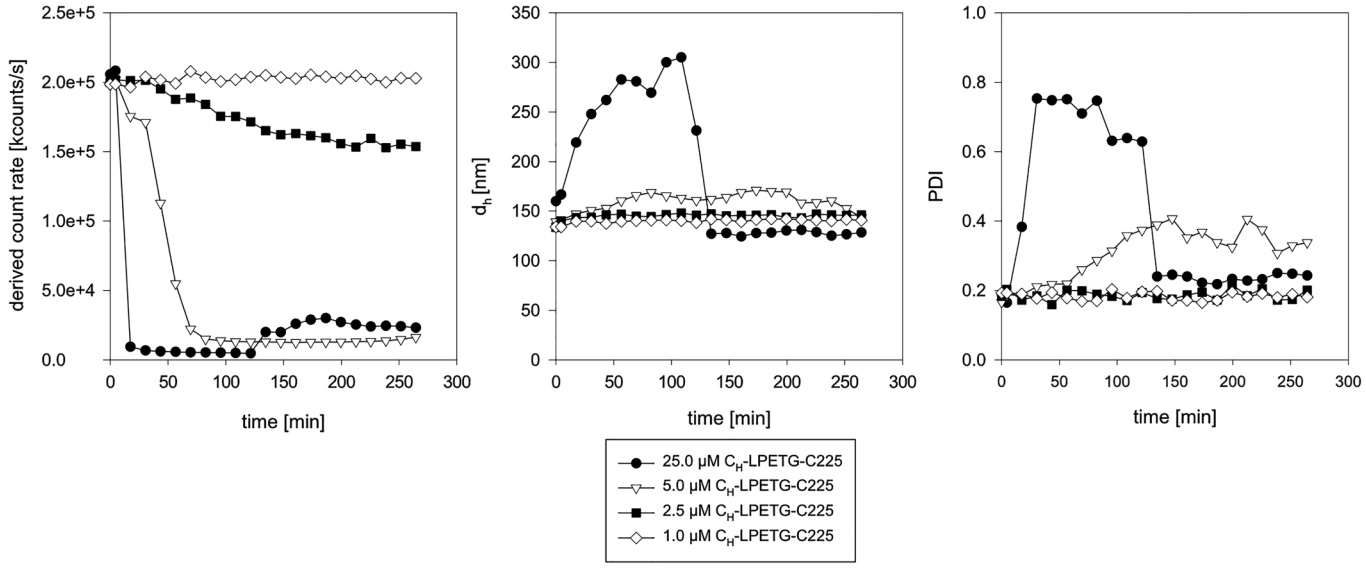

Fig. 5. Colloidal stability of the liposomal dispersion during sortagging. C_H–LPETG–C225 was spiked in different concentrations to 100 μM pentaglycine of DXR loaded liposomes and 25 μM Sortase-A. The reaction progress was monitored by dynamic light scattering for the derived count rate, hydrodynamic diameter and polydispersity index. Strong losses of light scattering intensity indicates aggregation and sedimentation during the reaction.

To gain deeper insights into the conjugation kinetic of C_H–LPETG–mAbs towards the pentaglycine modified surface of the PEGylated liposomes, the reaction of 1 μM C_H–LPETG–aHEL towards DXR–free liposomes was monitored over 14 h by rp–HPLC. Interestingly, the conversion followed a disproportionation profile (Fig. 6). Since the Sortase–A recognition motif LPETG is reformed during the reaction and, hence, also existing in the mAb-liposome product (Scheme 1), the latter can serve as a substrate for another reaction cycle. This reaction can either be the reverse reaction, which would result in deconjugation, or hydrolysis as a general side reaction of sortagging. For up to 4 h, the lipidation of C_H–LPETG–aHEL is the predominant reaction. After 4 h, most C_H–LPETG–aHEL was converted into (DMA-PEG)$_2$-C_H–LPETG–aHEL (56.3 ± 1.0 mol%), with a minor increase after a prolonged incubation to 14 h (61.8 ± 1.5 mol%). Compared to that, the (DMA-PEG)–C_H–LPETG–aHEL fraction reduced from 22.1 ± 3.2 mol% to 6.7 ± 0.5 mol% in the terminal reaction phase. Interestingly, unconjugated C_H–LPETG–aHEL fraction showed an increase from 21.0 ± 0.5 mol% to 30.5 ± 2.6 mol% between 4 h and 14 h. C_H–LPET-aHEL lacking the hydrolyzed terminal glycine is expected to elute with intact C_H–LPETG–aHEL in the rp–HPLC analysis (Fig. 4). Thus, the reaction kinetic indicated that not the di-modification, but a hydrolytic cleavage of (DMA-PEG)–C_H–LPETG–aHEL towards C_H-LPET-aHEL was predominant in the terminal phase of the reaction. The prolonged incubation therefore especially impacts the fraction of mono-modified mAb and reduces the total amount of ligand conjugated to the liposomes. On the other hand, a prolonged sortagging reaction improves chemical homogeneity of the obtained immunoliposomes, since the intermediate (DMA-PEG)–C_H–LPETG–aHEL fraction is reduced compared to the final product (DMA-PEG)$_2$–C_H–LPETG–aHEL.

Summarizing the investigations on reaction conditions and kinetics, it can be concluded that the initial concentration of C_H–LPETG–aHEL should not exceed 2.5 μM to prevent extensive aggregation of the liposomal dispersion at the investigated conditions (4 °C incubation temperature, 25 μM Sortase–A, 100 μM pentaglycine). The kinetic investigations identified that the maximal amount (78.4 mol% of 1 μM) was conjugated to the PEGylated liposomes after 4 h, either as mono- or di-modified variant. Hence, these conditions were chosen to prepare DXR-loaded immunoliposomes for in vitro cytotoxicity tests.

4.3. In vitro cytotoxicity of targeted DXR-liposomes on breast cancer cells

In order to evaluate if doxorubicin encapsulation in functionalized liposomes simultaneously mediated decreased unspecific toxicity but increased targeted activity against EGFR$^+$ cells, we performed in vitro cytotoxicity assays. DPPC based, DXR loaded liposomes were modified with 1.0 or 2.5 μM C_H–LPETG–aHEL or C_H–LPETG–C225, respectively, and purified by dialysis. For that purpose, a dialysis device with a membrane molecular weight cut–off of 1000 kDa was chosen, which should ensure a sufficient permeability for Sortase–A (20.9 kDa) as well as monoclonal antibodies (C_H–LPETG–aHEL: 146.1 kDa, C_H–LPETG–C225: 146.7 kDa). Furthermore, these devices were previously reported to retain the nanoparticulate liposome dispersion in a sufficient manner (lipid recovery > 88%, [31]). DPPC-based liposomes modified with 1.0 or 2.5 μM C_H–LPETG–C225 or C_H–LPETG–aHEL showed neither changes in the hydrodynamic diameter nor in PDI (Table 1) after the final liposome processing compared to the non-conjugated control. No macroscopically visible precipitation or lipid loss (data not shown) was observed.

EGFR$^+$ MDA–MB–468 cells were exposed to the dialyzed formulations for 4 h and, after careful medium exchange, incubated for another 3 days in pure growth medium. It should be tested whether the drug encapsulation could first decrease the unspecific toxicity of pure doxorubicin, and second, whether a selective targeting via the EGF-receptor was able to re-increase the cytotoxicity in vitro (Fig. 7). Pure doxorubicin had an IC_{50} of 0.3 ± 1.2 μg/mL (Fig. 8), which is in line with previously reported IC_{50} values on this cell line (Mamot et al: 0.8 μg/mL [40]). Encapsulation of DXR in the pentaglycine modified, PEGylated liposomes (DPPC–LS) led to an 18fold decrease of toxicity as indicated by an appropriate increase in IC_{50} (Fig. 8A). Similar values were obtained for the isotype-control C_H–LPETG–aHEL carrying immunoliposomes (19fold and 21fold increase for 1.5 μM-aHEL-DPPC-LS and 2.5 μM-aHEL-DPPC-LS, respectively; not significantly different from mAb–free DPPC-LS). Drug-free (empty) liposomes were not toxic (tested up to 1.3 mM total lipid, Fig. 7). Conjugation of C_H–LPETG–C225 mediated an increased cytotoxicity of the liposomes to an IC_{50} of 3.2 μg/mL for 1.0 μM-C225-DPPC-LS and 2.2 μg/mL for 2.5 μM-C225-DPPC-LS, latter significantly different from DPPC–LS ($p < 0.05$, Fig. 8A). This indicates a targeted cytotoxicity, that is further amplified at higher ligand densities. Cellular specificity, meaning selective toxicity of C225-targeted liposomes on EGFR-over-expressing cells, but equal toxicity of targeted and non-targeted liposomes on EGFR$^-$ cells has been demonstrated several times with comparable liposomal constructs [40,43] or C225-based ADCs [24]. The here presented targeted cytotoxicity was also not due to synergistic effects of C_H–LPETG–C225 and liposomal doxorubicin, as a physical mixture (C_H–LPETG–C225: DXR ratio equal to 2.5 μM-C225-DPPC-LS) showed cytotoxicity comparable to the isotype- or unconjugated liposomes. This underlines the requirement of a stable (covalent) anchoring of the ligand onto the targeted drug delivery system.

Previous reports suggested a density of 0.3–1.2 nM ligand/μM phospholipid for C225 Fab' targeted DXR liposomes, reaching IC_{50} values of 1.1 μg/mL on the same cell line [38,40]. The ligand density of the presented liposomes ranged from 0.05–0.15 nM ligand/μM phospholipid (Table 1). For direct comparison it should be considered, that monoclonal antibodies provide two ligand binding sites compared to a Fab' fragment. Interestingly, we found only slightly higher IC_{50} values for the 2.5 μM-C225-DPPC-LS constructs (1.1 μg/mL described by Mamot et al. versus 2.2 μg/mL described here). However, more drastic differences were observed for untargeted DPPC–LS (32 μg/mL versus 5.8 μg/mL).

The higher unspecific toxicity of the presented system led to the question whether the particle shape or usage of DPPC (instead of the

Table 1
Physico-chemical parameters of EGFR targeted DXR-liposomes and control groups (standard deviation shown for triplicate analyses).

Formulation	d_h [nm]	PDI	zp [mV]	DXR:mAb ratio	nM mAB/μM PL
DPPC-LS	142 + 1	0.19 + 0.03	−9.3 + 0.5	–	–
1.0 μM-aHEL-DPPC-LS	143 + 1	0.19 + 0.01	−7.5 + 0.4	5982	0.057
2.5 μM-aHEL-DPPC-LS	144 + 0	0.20 + 0.00	−5.3 + 0.8	2418	0.138
1.0 μM-C225-DPPC-LS	143 + 1	0.20 + 0.01	−8.0 + 0.3	6334	0.053
2.5 μM-C225-DPPC-LS	145 + 1	0.19 + 0.02	−7.2 + 0.2	2327	0.147
HSPC-LS	120 + 1	0.22 + 0.00	−14.8 + 0.6	–	–
1.0 μM-aHEL-HSPC-LS	101 + 2	0.23 + 0.01	−12.6 + 0.3	4911	0.072
1.0 μM-C225-HSPC-LS	121 + 1	0.22 + 0.01	−10.7 + 0.2	5732	0.062

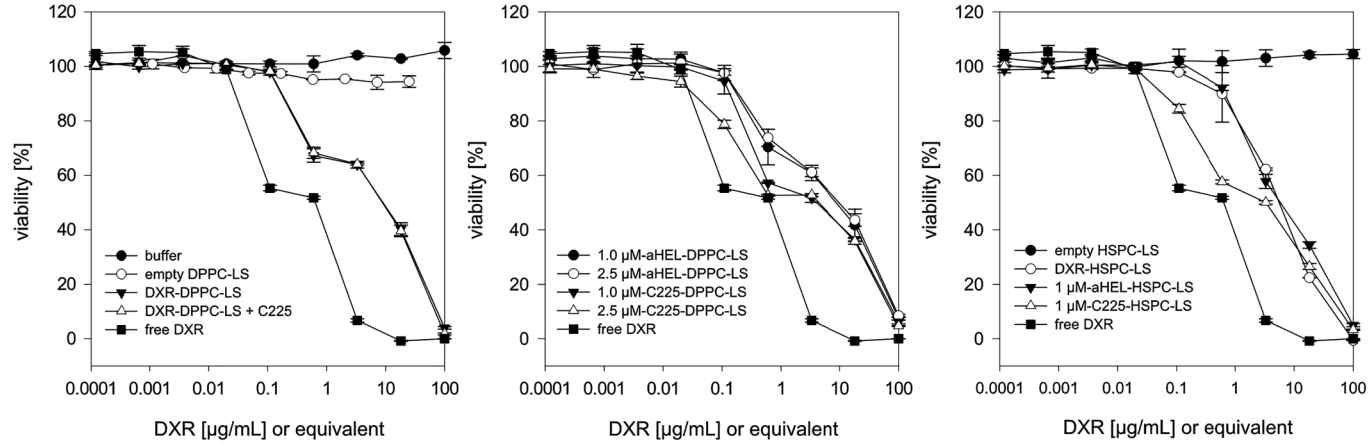

Fig. 7. Viability curves of targeted, DXR-loaded DPPC-LS, HSPC-LS and controls. MDA-MB-468 cells were incubated with the liposomal formulations at different DXR concentrations (or equivalent lipid concentrations, according to the DXR:lipid ratio of drug loaded LS). After 4 h, medium containing unbound liposomes was exchanged, followed by a further incubation of the cells for 3 days, until viability was assessed. Free DXR showed highest cytotoxicity, what could be alleviated by drug encapsulation. EGFR targeting led to a re-increase of cytotoxicity.

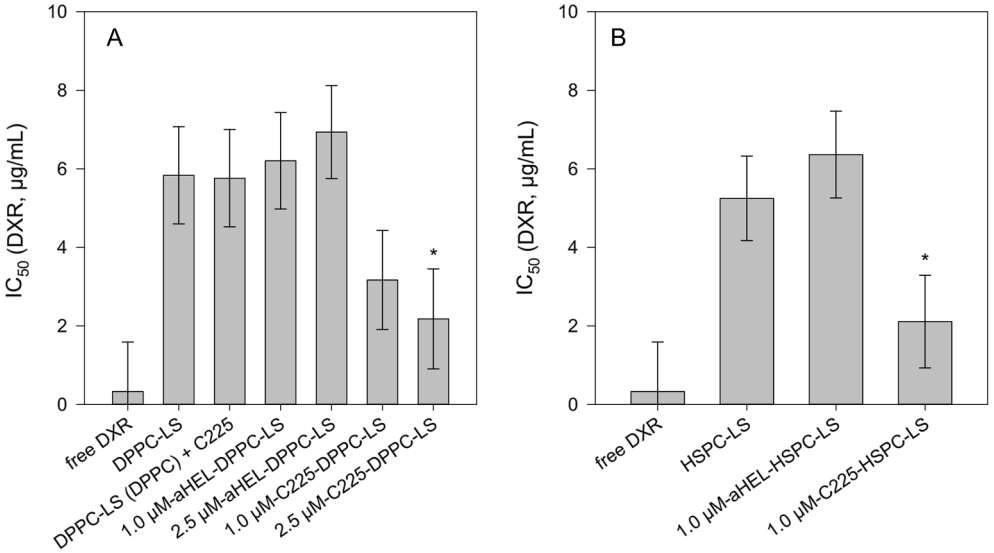

Fig. 8. IC_{50} values of EGFR targeted, DXR loaded liposomes and controls on MDA-MB-468 cells (data is shown as mean ± standard deviation of two biological experiments; * indicates significant differences ($p < 0.05$) to the ligand free control). A: DPPC–based liposomes, loaded with DXR from DPBS buffer and showing significant rod-like morphology. B: HSPC-based liposomes, loaded with DXR from HEPES buffer and assumed to have a predominant "coffee-bean" structure. Targeted formulations increased cytotoxicity over non-targeted ones. No relevant differences were observed between the DPPC and HSPC based formulations.

higher melting HSPC) was the reason for this observation. We therefore prepared HPSC-based liposomes (HSPC-LS) which were loaded with DXR from HEPES buffer to achieve a predominant "coffee–bean" shape based on our morphological investigations (Fig. 3) and previously reported cryo-TEM analysis of comparably prepared liposomes [42]. An overview of the different liposomal preparation conditions, the corresponding morphological analyses and link to cytotoxicity read–out is given in Supplementary Table 1. The HSPC-LS were then conjugated with either 1.0 or 2.5 µM C_H–LPETG–aHEL or C_H–LPETG–C225. The reaction behavior was found to be less stable in HEPES compared to DPBS, as strong precipitation was observed for the 2.5 µM group, which was therefore not considered for in vitro analyses. Minor aggregates in the 1.0 µM group were removed by centrifugation (5 min at 800 × g), leading to a lipid loss of 10–25% (data not shown). Interestingly, negligible impact on IC_{50} values compared to DPPC-LS was observed (5.3 ± 1.1, 6.4 ± 1.1 and 2.1 ± 1.2 µg/mL for ligand free, C_H–LPETG–aHEL and C_H–LPETG–C225-modifed liposomes, respectively; Fig. 8B). This suggests a minor influence of DPPC or HSPC usage and also DXR-loading procedure on the in vitro performance. The non-targeted DPPC- and HSPC–based formulations showed no significant differences of unspecific toxicity that could have been caused by the different morphology or bilayer rigidity. The unspecific toxicity was unexpectedly high, expressed in a ratio of 2.5 between the IC_{50} value of non-targeted HSPC–LS and 1.0 µM–C225–HSPC–LS. Mamot et al. reported a ratio of 29 between comparably composed targeted or non-targeted liposomes on the same cell line [40]. This difference may be explained by different cytotoxicity experiment settings. Especially the longer exposition of cells (2 h in literature compared to 4 h in the presented report) to the liposomes prior the wash-out may have led to a drug release and hence higher unspecific toxicity. Comparable observations were previously reported for CD19-targeted, DXR loaded liposomes [44]. Although the authors obtained only low ratios of 4.6 (for 1 h incubation of cells with the liposomes) or 1.8 (for 24 h incubation) in vitro, the targeted liposomes were able to significantly enhance the mean survival time of B–lymphoma model mice. Comparably, Zalba et al. reported a low ratio of 1.5 between the IC_{50} of EGFR-targeted (26 µM) or non-targeted (39 µM), oxaliplatin loaded liposomes on SW-480 cells (colorectal cancer cells) after 4 h incubation. Nevertheless, the targeted liposomes clearly improved tumor growth inhibition of SW–480 derived xenografts in mice compared to non–targeted ones [43]. These results underline that low ratios in IC_{50} values between targeted and non-targeted liposomes observed in vitro are not necessarily predictive for the in vivo performance of the drug delivery system.

5. Conclusion and outlook

In the presented work, we thoroughly investigated the loading of doxorubicin into pentaglycine modified liposomes which were prepared in a controllable and scalable manufacturing process. The pentaglycine lipid anchor was used to conjugate C_H–LPETG–mAbs as targeting ligands on the drug delivery system by sortagging. The conjugation required detailed analyses of reaction conditions and kinetics, as a strong aggregation and precipitation propensity was observed. This was attributed to the presence of two LPETG-motifs per mAb that may lead to cross–linking between liposomes. Precipitation was circumvented by a drastic reduction of the C_H–LPETG–mAb: lipid ratio during reaction. This decrease consequently led to decreased ligand densities < 0.3 nM/μM PL on the liposomal system. Although the ligand density was low, the liposomal drug delivery system could increase the specificity of doxorubicin toxicity in vitro in a targeted manner. This was firstly indicated by an 18fold increase of the IC_{50} by drug encapsulation in the carrier. Secondly, grafting of cetuximab on the liposomal surface led to a re-decrease of the IC_{50} on breast cancer cells carrying the targeted structure. This drug targeting effect was ligand specific since it was not shown by liposomes functionalized with an isotype control antibody. Increased ligand density may further improve binding efficacy and internalization of the liposomal system [40], which is known to be more effective if multivalent (binding of several receptors) systems are used [45]. Therefore, the use of alternative sortaggable ligands such as Fab's, single-chain fragment variables (scFv) or single–domain antibodies employed with a single LPxTG–motif should be considered for optimization. This would firstly reduce the mass per ligand conjugated to the carrier and secondly avoid liposome cross–linking during conjugation. Furthermore, usage of ligands lacking a Fc-domain would also circumvent pharmacokinetic disadvantages known from full length mAbs used as targeting ligands for immunoliposomes [43,46–49].

Whether such EGFR-targeted, DXR loaded drug carriers may improve the treatment of solid tumors in humans was recently investigated in a phase I trial [3]. Interestingly, the authors reported a remarkably low skin cytotoxicity, an issue which is a major concern in the development of EGFR-targeted ADCs [24]. This observation may strengthen the consideration of particulate targeting systems, such as the described nano–sized liposomal system as an alternative to antibody-drug conjugates.

Declarations of interest

The company Merck KGaA, Darmstadt, Germany owns manufacturing and distribution rights for cetuximab (Erbitux®) outside the USA and Canada.

Acknowledgement

The authors would like to thank Christopher Bachran and Lee Kim Swee from BioMed X GmbH for supply of Sortase-A. Martina Jeschke is gratefully acknowledged for support during liposome manufacturing. Furthermore, the authors like to thank Markus Drechsler from University of Bayreuth for cryo–TEM pictures.

Appendix A. Supplementary material

Supplementary data to this article can be found online at https://doi.org/10.1016/j.ejpb.2019.01.020.

References

[1] M. Merino, S. Zalba, M.J. Garrido, Immunoliposomes in clinical oncology: state of the art and future perspectives, J. Control. Release (2018).
[2] P. Marques-Gallego, A.I. de Kroon, Ligation strategies for targeting liposomal nanocarriers, Biomed. Res. Int. 2014 (2014) 129458.
[3] C. Mamot, R. Ritschard, A. Wicki, G. Stehle, T. Dieterle, L. Bubendorf, C. Hilker, S. Deuster, R. Herrmann, C. Rochlitz, Tolerability, safety, pharmacokinetics, and efficacy of doxorubicin-loaded anti-EGFR immunoliposomes in advanced solid tumours: a phase 1 dose-escalation study, Lancet Oncol. 13 (2012) 1234–1241.
[4] Y. Matsumura, M. Gotoh, K. Muro, Y. Yamada, K. Shirao, Y. Shimada, M. Okuwa, S. Matsumoto, Y. Miyata, H. Ohkura, K. Chin, S. Baba, T. Yamao, A. Kannami, Y. Takamatsu, K. Ito, K. Takahashi, Phase I and pharmacokinetic study of MCC-465, a doxorubicin (DXR) encapsulated in PEG immunoliposome, in patients with metastatic stomach cancer, Ann. Oncol. 15 (2004) 517–525.
[5] P.N. Munster, K. Miller, I.E. Krop, N. Dhindsa, J. Reynolds, E. Geretti, C. Niyikiza, U. Nielsen, B. Hendriks, T.J. Wickham, V.M. Moyo, P. LoRusso, A phase I study of MM-302, a HER2-targeted liposomal doxorubicin, in patients with advanced, HER2-positive (HER2+) breast cancer, J. Clin. Oncol. 30 (2012) TPS663-TPS663.
[6] Y. Barenholz, Doxil® — The first FDA-approved nano-drug: lessons learned, J. Control. Release 160 (2012) 117–134.
[7] A.N. Lukyanov, T.A. Elbayoumi, A.R. Chakilam, V.P. Torchilin, Tumor-targeted liposomes: doxorubicin-loaded long-circulating liposomes modified with anti-cancer antibody, J. Control. Release 100 (2004) 135–144.
[8] S.C. Alley, D.R. Benjamin, S.C. Jeffrey, N.M. Okeley, D.L. Meyer, R.J. Sanderson, P.D. Senter, Contribution of linker stability to the activities of anticancer immunoconjugates, Bioconjugate Chem. 19 (2008) 759–765.
[9] N. Jain, S.W. Smith, S. Ghone, B. Tomczuk, Current ADC linker chemistry, Pharm. Res. 32 (2015) 3526–3540.
[10] M. Ritzefeld, Sortagging: A robust and efficient chemoenzymatic ligation strategy, Chem. – A Eur. J. 20 (2014) 8516–8529.
[11] R.R. Beerli, T. Hell, A.S. Merkel, U. Grawunder, Sortase enzyme-mediated generation of site-specifically conjugated antibody drug conjugates with high in vitro and in vivo potency, PLOS ONE 10 (2015) e0131177.
[12] L.S. Lee, C. Conover, C. Shi, M. Whitlow, D. Filpula, Prolonged circulating lives of single-chain Fv proteins conjugated with polyethylene glycol: a comparison of conjugation chemistries and compounds, Bioconjugate Chem. 10 (1999) 973–981.
[13] J. Guo, S. Kumar, M. Chipley, O. Marcq, D. Gupta, Z. Jin, D.S. Tomar, C. Swabowski, J. Smith, J.A. Starkey, S.K. Singh, Characterization and Higher-order structure assessment of an interchain cysteine-based ADC: impact of drug loading and distribution on the mechanism of aggregation, Bioconjugate Chem. 27 (2016) 604–615.
[14] Y.T. Adem, K.A. Schwarz, E. Duenas, T.W. Patapoff, W.J. Galush, O. Esue, Auristatin antibody drug conjugate physical instability and the role of drug payload, Bioconjugate Chem. 25 (2014) 656–664.
[15] O. Tacar, P. Sriamornsak, C.R. Dass, Doxorubicin: an update on anticancer molecular action, toxicity and novel drug delivery systems, J. Pharm. Pharmacol. 65 (2013) 157–170.
[16] M. Theodoulou, C. Hudis, Cardiac profiles of liposomal anthracyclines, Cancer 100 (2004) 2052–2063.
[17] J. Gubernator, Active methods of drug loading into liposomes: recent strategies for stable drug entrapment and increased in vivo activity, Exp. Opin. Drug Delivery 8 (2011) 565–580.
[18] A. Gabizon, R. Catane, B. Uziely, B. Kaufman, T. Safra, R. Cohen, F. Martin, A. Huang, Y. Barenholz, Prolonged circulation time and enhanced accumulation in malignant exudates of doxorubicin encapsulated in polyethylene-glycol coated liposomes, Cancer Res. 54 (1994) 987.
[19] Z. Symon, D. Peyser A Fau - Tzemach, O. Tzemach D Fau - Lyass, E. Lyass O Fau - Sucher, E. Sucher E Fau - Shezen, A. Shezen E Fau - Gabizon, A. Gabizon, Selective delivery of doxorubicin to patients with breast carcinoma metastases by stealth liposomes, Cancer, 86 (1999) 72-78.
[20] R. Solomon, A.A. Gabizon, Clinical pharmacology of liposomal anthracyclines: focus on pegylated liposomal doxorubicin, Clin. Lymphoma Myeloma 8 (2008) 21–32.
[21] C. Yewale, D. Baradia, I. Vhora, S. Patil, A. Misra, Epidermal growth factor receptor targeting in cancer: a review of trends and strategies, Biomaterials 34 (2013) 8690–8707.
[22] K.M. Riaz, A.M. Riaz, X. Zhang, C. Lin, H.K. Wong, X. Chen, G. Zhang, A. Lu, Z. Yang, Surface functionalization and targeting strategies of liposomes in solid tumor therapy: a review, Int. J. Molec. Sci. 19 (2018).
[23] J. Tol, C.J.A. Punt, Monoclonal antibodies in the treatment of metastatic colorectal cancer: a review, Clin. Therap. 32 (2010) 437–453.
[24] C. Sellmann, A. Doerner, C. Knuehl, N. Rasche, V. Sood, S. Krah, L. Rhiel, A. Messemer, J. Wesolowski, M. Schuette, S. Becker, L. Toleikis, H. Kolmar, B. Hock, Balancing selectivity and efficacy of bispecific epidermal growth factor receptor (EGFR) × c-MET antibodies and antibody-drug conjugates, J. Biol. Chem. 291 (2016) 25106–25119.
[25] S. Wöll, S. Schiller, C. Bachran, L.K. Swee, R. Scherließ, Pentaglycine lipid derivates – rp-HPLC analytics for bioorthogonal anchor molecules in targeted, multiple-composite liposomal drug delivery systems, Int. J. Pharm. 547 (2018) 602–610.
[26] C. Bachran, M. Schröder, L. Conrad, J.J. Cragnolini, F.G. Tafesse, L. Helming, H.L. Ploegh, L.K. Swee, The activity of myeloid cell-specific VHH immunotoxins is target-, epitope-, subset- and organ dependent, Sci. Rep. 7 (2017) 17916.
[27] S. Wöll, C. Bachran, S. Schiller, M. Schröder, L. Conrad, L. Kim Swee, R. Scherließ, Sortaggable liposomes: Evaluation of reaction conditions for single-domain antibody conjugation by Sortase–A and targeting of CD11b+ myeloid cells, Eur. J. Pharm. Biopharm. 133 (2018) 138–150.
[28] G. Haran, R. Cohen, L.K. Bar, Y. Barenholz, Transmembrane ammonium sulfate gradients in liposomes produce efficient and stable entrapment of amphipathic weak bases, Biochimica et Biophysica Acta (BBA)-Biomembranes 1151 (1993) 201–215.

[29] A. Klaiber, C. Lanz, S. Landsmann, J. Gehring, M. Drechsler, S. Polarz, Maximizing headgroup repulsion: hybrid surfactants with ultrahighly charged inorganic heads and their unusual self-assembly, Langmuir: ACS J. Surf. Colloids 32 (2016) 10920–10927.
[30] D. Carugo, E. Bottaro, J. Owen, E. Stride, C. Nastruzzi, Liposome production by microfluidics: potential and limiting factors, Sci. Rep. 6 (2016) 25876.
[31] S. Wöll, C. Bachran, S. Schiller, M. Schröder, L. Conrad, R. Scherließ, L.K. Swee, Sortagging of liposomes with a murine CD11b-specific VHH increases in vitro and in vivo targeting specificity of myeloid cells, Eur. J. Pharm. Biopharm. 134 (2019) 190–198.
[32] R.L. Biltonen, D. Lichtenberg, The use of differential scanning calorimetry as a tool to characterize liposome preparations, Chem. Phys. Lipids 64 (1993) 129–142.
[33] A. Fritze, F. Hens, A. Kimpfler, R. Schubert, R. Peschka-Süss, Remote loading of doxorubicin into liposomes driven by a transmembrane phosphate gradient, Biochimica et Biophysica Acta (BBA) - Biomembranes 1758 (2006) 1633–1640.
[34] N. Ohnishi, H. Tomida, Y. Ito, K. Tahara, H. Takeuchi, Characterization of a doxorubicin liposome formulation by a novel in vitro release test methodology using column-switching high-performance liquid chromatography, Chem. Pharm. Bull. 62 (2014) 538–544.
[35] Diafiltration (Buffer Exchange) Using Hollow Fiber Membranes instead of Dialysis Tubing – Automated Diafiltration, http://spectrumlabs.com/lit/hfdial.pdf, undeclared publication year (accessed on 04.03.2018).
[36] D.D. Lasic, P.M. Frederik, M.C.A. Stuart, Y. Barenholz, T.J. McIntosh, Gelation of liposome interior A novel method for drug encapsulation, FEBS Letters 312 (1992) 255–258.
[37] D.D. Lasic, R. Joannic, B.C. Keller, P.M. Frederik, L. Auvray, Spontaneous vesiculation, Adv. Colloid Interf. Sci. 89–90 (2001) 337–349.
[38] C. Mamot, D.C. Drummond, C.O. Noble, V. Kallab, Z. Guo, K. Hong, D.B. Kirpotin, J.W. Park, Epidermal growth factor receptor-targeted immunoliposomes significantly enhance the efficacy of multiple anticancer drugs in vivo, Cancer Res. 65 (2005).
[39] K. Kono, M. Takashima, E. Yuba, A. Harada, Y. Hiramatsu, H. Kitagawa, T. Otani, K. Maruyama, S. Aoshima, Multifunctional liposomes having target specificity, temperature-triggered release, and near-infrared fluorescence imaging for tumor-specific chemotherapy, J. Control. Release (2015).
[40] C. Mamot, D.C. Drummond, U. Greiser, K. Hong, D.B. Kirpotin, J.D. Marks, J.W. Park, Epidermal Growth Factor Receptor (EGFR)-targeted immunoliposomes mediate specific and efficient drug delivery to EGFR- and EGFRvIII-overexpressing tumor cells, Cancer Res. 63 (2003) 3154.
[41] R.M. Schiffelers, G.A. Koning, T.L.M. ten Hagen, M.H.A.M. Fens, A.J. Schraa, A.P.C.A. Janssen, R.J. Kok, G. Molema, G. Storm, Anti-tumor efficacy of tumor vasculature-targeted liposomal doxorubicin, J. Control. Release 91 (2003) 115–122.
[42] T. Li, D. Cipolla, T. Rades, B.J. Boyd, Drug nanocrystallisation within liposomes, J. Control. Release (2018).
[43] S. Zalba, A.M. Contreras, A. Haeri, T.L.M. ten Hagen, I. Navarro, G. Koning, M.J. Garrido, Cetuximab-oxaliplatin-liposomes for epidermal growth factor receptor targeted chemotherapy of colorectal cancer, J. Control. Release 210 (2015) 26–38.
[44] D.L. Iden, T.M. Allen, In vitro and in vivo comparison of immunoliposomes made by conventional coupling techniques with those made by a new post-insertion approach, Biochimica et Biophysica Acta (BBA) - Biomembranes 1513 (2001) 207–216.
[45] S. Oliveira, R.M. Schiffelers, J. van der Veeken, R. van der Meel, R. Vongpromek, PM.P. van Bergen en Henegouwen, G. Storm, C. Roovers, Downregulation of EGFR by a novel multivalent nanobody-liposome platform, J. Control. Release 145 (2010) 165–175.
[46] W.W.K. Cheng, T.M. Allen, Targeted delivery of anti-CD19 liposomal doxorubicin in B-cell lymphoma: a comparison of whole monoclonal antibody, Fab′ fragments and single chain Fv, J. Control. Release 126 (2008) 50–58.
[47] F. Pastorino, C. Brignole, D. Marimpietri, P. Sapra, E.H. Moase, T.M. Allen, M. Ponzoni, Doxorubicin-loaded Fab′ Fragments of Anti-disialoganglioside Immunoliposomes selectively inhibit the growth and dissemination of human neuroblastoma in nude mice, Cancer Res. 63 (2003) 86.
[48] P. Sapra, T.M. Allen, Improved outcome when B-cell lymphoma is treated with combinations of immunoliposomal anticancer drugs targeted to both the CD19 and CD20 epitopes, Clin. Cancer Res. 10 (2004) 2530–2537.
[49] P. Simard, J.-C. Leroux, In vivo evaluation of pH-sensitive polymer-based immunoliposomes targeting the CD33 antigen, Molecular Pharm. 7 (2010) 1098–1107.